



Published in final edited form as:

*Transl Stroke Res.* 2022 June ; 13(3): 494–504. doi:10.1007/s12975-021-00955-9.

## Bone marrow derived *Alk1* mutant endothelial cells and clonally expanded somatic *Alk1* mutant endothelial cells contribute to the development of brain arteriovenous malformations in mice

Sonali S. Shaligram<sup>1,2</sup>, Rui Zhang<sup>1,2</sup>, Wan Zhu<sup>1,2</sup>, Li Ma<sup>1,2</sup>, Man Luo<sup>1,2</sup>, Qiang Li<sup>3</sup>, Miriam Weiss<sup>3</sup>, Thomas Arnold<sup>4</sup>, NG Santander Grez<sup>4</sup>, Rich Liang<sup>1,2</sup>, Leandro do Prado<sup>1,2</sup>, Chaoliang Tang<sup>1,2</sup>, Felix Pan<sup>1,2</sup>, S. Paul Oh<sup>5</sup>, Peipei Pan<sup>1,2</sup>, Hua Su<sup>1,2,6</sup>

<sup>1</sup>Center for Cerebrovascular Research, University of California, San Francisco, California, USA.

<sup>2</sup>Department of Anesthesia and Perioperative Care, University of California, San Francisco, California, USA.

<sup>3</sup>Department of Neurosurgery, University of California, San Francisco, California, USA.

<sup>4</sup>Department of Pediatrics, University of California, San Francisco, California, USA

<sup>5</sup>Barrow Aneurysm & AVM Research Center, Department of Neurobiology, Barrow Neurological Institute, Phoenix, Arizona, USA

### Abstract

Homozygous mutation in arteriovenous malformation (AVM) causative genes in a fraction of endothelial cells (ECs) causes brain AVMs (bAVMs). Heterozygous mutation of an AVM causative gene, endoglin, in bone marrow (BM) caused capillary dysplasia in mouse brain. We hypothesize that homozygous mutation of activin receptor-like kinase 1 (*Alk1*, another AVM causative gene) in BM derived ECs (BMDECs) is sufficient to cause bAVM in brain angiogenic region, *Alk1*<sup>-</sup> ECs can clonally expand in bAVM, and the burden of *Alk1*<sup>-</sup> ECs correlates with bAVM severity. The BMs of *Pdgfβ*CreER;*Alk1*<sup>2f/2f</sup>;Ai14 mice with EC-specific tamoxifeninducible Cre and *Alk1* floxed alleles were transplanted into wild-type mice to analyze the role of BMDECs in bAVM development. *Pdgfβ*CreER;*Alk1*<sup>2f/2f</sup>;confetti<sup>+/-</sup> mice with Cre-regulated confetti transgene were used to study EC clonal expansion. bAVMs were induced by intra-brain injection of an adeno-associated viral vector expressing vascular endothelial growth factor followed with intra-peritoneal injection of tamoxifen. Wild-type mice transplanted with *Pdgfβ*CreER;*Alk1*<sup>2f/2f</sup>;Ai14 BM developed bAVMs after bAVM induction. Recombined BMDECs were detected in bAVMs. The presence of clusters of ECs expressing same confetti

<sup>6</sup>Hua Su, MD, Department of Anesthesia and Perioperative Care, University of California, San Francisco, 1001 Potrero Avenue, Box 1363, San Francisco, CA 94110, Phone: 415-206-3162, Fax: 415-206-8907, hua.su@ucsf.edu.

Authors' contribution

HS, SS and TA designed the experiment, SS, ML, QL, RZ, LM, MW, SNG, RL, LP, CT, and FP collected and analyzed the data, SS, HS drafted the manuscript, TA, PP, SPO, HS critically read the manuscript.

Conflicts of interests

The authors do not have competing interests.

Ethics approval

The protocol and experimental procedures for using laboratory animals were approved by the Institution of Animal Care and Use Committee (IACUC) at the University of California, San Francisco.

color in bAVMs suggests that  $Alk1^{-}$  ECs have been clonally expanded. Increasing tamoxifen dose increased the number of  $Alk1^{-}$  ECs and abnormal vessels in bAVMs of *PdgfbiCreER;Alk1<sup>2f/2f</sup>* mice. Our data indicated that homozygous mutation of *Alk1* in BMDECs is sufficient to cause bAVM development in brain angiogenic region; clonal expansion of  $Alk1^{-}$  ECs provides a likely mechanism for how a fraction of mutant ECs causes bAVM; and the burden of  $Alk1^{-}$  ECs correlates with AVM severity.

## Keywords

arteriovenous malformation; *Alk1*; endothelial cells; clonal expansion; bone marrow derived endothelial cells

## INTRODUCTION

Arteriovenous malformations (AVMs) are tangles of abnormal vessels that shunt blood directly from arteries to veins. Vessels in AVM have abnormal wall structure and are prone to rupture causing life-threatening hemorrhage [1]. Most AVM cases are sporadic [2]. There are a few rare inherited diseases that feature AVMs, such as hereditary hemorrhagic telangiectasia (HHT), an autosomal dominant disorder caused by mutations in endoglin (*ENG*), activin receptor-like kinase 1 (*ALK1* also known as *ACVLR1*), and *SMAD4* [3, 4]. HHT patients have a high prevalence of telangiectasias in the skin and gastrointestinal mucosa, and AVMs in multiple organs including the brain, lung, and liver. Although HHT causal genes are mostly identified, the mechanisms of AVM development are largely unknown [2].

We have established several HHT AVM mouse models that have the AVMs in multiple organs and in the brain angiogenic region through conditional deletion of *Eng* or *Alk1* in adult mice, combined with brain focal angiogenic stimulation [5–8]. Using these models, we found that both mutation of *Alk1* or *Eng* in the endothelial cells (ECs) and focal angiogenic stimulation are necessary for AVM development in the brain of adult mouse [6, 7, 9]. Mutation of *Alk1* or *Eng* in ECs is also necessary for AVM development in other organs [10]. We also found that homozygous mutation of *Alk1* or *Eng* in a fraction of somatic ECs [5, 11] is sufficient to induce brain AVMs (bAVMs) and arteriovenous (AV) shunts in the intestines of adult mice. Bone marrow (BM) derived cells have been detected in brain angiogenic region [12]. We have shown that transplantation of BM cells with heterozygous mutation of *Eng* (+/-) caused capillary dysplasia in brain angiogenic regions of wild-type (WT) mice [13], suggesting a potential contribution of BM-derived cells to the pathogenesis of vascular malformation. However, it is not clear how a small fraction of mutant ECs leads to AVM, and if mutation of AVM causative genes in BM-derived ECs (BMDECs) alone can cause AVM.

EC *Eng* mutation in neonates increases proliferation of both  $Eng^{-}$  and  $Eng^{+}$  ECs in AVM vessels [14]. We found that proliferating  $Alk1^{-}$  ECs preferentially cluster in bAVM vessels [7]. It spurs an idea that the small numbers of ECs with biallelic loss of *ALK1* can clonally overpopulate. We used the R26R-confetti reporter [15] to determine if  $Alk1^{-}$  ECs are undergoing clonal expansion in bAVMs. Confetti mice carry four fluorescent proteins

–green fluorescent protein (GFP), red fluorescent protein (RFP), yellow fluorescent protein (YFP) and cyan fluorescent protein (CFP). Tamoxifen (TM) treatment will trigger Cre expression which will activate the expression of 1 of the 4 confetti fluorescent genes in individual cells. The progenies of these cells will express the same fluorescent protein. Thus, this reporter provides a unique way to identify a cluster of cells that are derived from a single parental cell, demonstrating clonal expansion [16].

In this paper, we found that homozygous mutation of *Alk1* in BMDECs alone is sufficient for bAVM development. We also found that *Alk1*<sup>-</sup> ECs were clonally expanded in bAVMs, and the number of *Alk1*<sup>-</sup> ECs was positively correlated with AVM phenotype severity.

## MATERIALS AND METHODS

### Animals

The protocol and experimental procedures for using laboratory animals were approved by the Institution of Animal Care and Use Committee (IACUC) at the University of California, San Francisco. Animal husbandry was provided by the staff of the IACUC, under the guidance of supervisors who are certified Animal Technologists, and by the staff of the Animal Core Facility. Veterinary care was provided by IACUC faculties and veterinary residents located on the Zuckerberg San Francisco General Hospital campus.

*PdgfbiCreER;Alk1<sup>2f/2f</sup>;Ai14<sup>+/-</sup>* mice that express an EC-specific TM inducible Cre recombinase, have their *Alk1* gene exons 4–6 floxed [17], and carry the Ai14 reporter were used as BM donors and in other experiments. C57BL/6J and C57BL/6-Tg(CAG-EGFP)10sb/J mice (the Jackson Laboratory, Bar Harbor, ME) were used as BM recipients and donors.

*PdgfbiCreER;Alk1<sup>2f/2f</sup>;confetti<sup>+/-</sup>* mice that carry the R26R-confetti Cre-regulated transgene were used to test the clonal expansion of *Alk1*<sup>-</sup> ECs. R26R-confetti transgene (*Gt(ROSA)26Sortm1(CAG-Brainbow2.1)Cle/J*, the Jackson Laboratory) has a loxP-flanked STOP cassette between the CAG promoter and the Confetti sequence. Confetti transgene contains two loxP-flanked dimers; one dimer has nuclear-localized GFP and reversed cytoplasmic YFP; the other dimer has cytoplasmic RFP and a reversed membrane-tethered CFP. *PdgfbiCreER;Alk1<sup>2f/2f</sup>;confetti<sup>+/-</sup>* mice were treated with a single intra-peritoneal (i.p.) injection of TM (2.5 mg/25g of body weight) to activate Cre expression in ECs, which deleted *Alk1* gene at the same time activated the expression of 1 of the 4 confetti colors in individual ECs. The individual fluorescent color is stably propagated within the progeny of each ECs [15].

The *PdgfbiCreER;Alk1<sup>2f/2f</sup>;Ai14<sup>+/-</sup>* mice were also treated with different doses of TM through single i.p. injections to induce different levels of *Alk1* gene deletion and Ai14 expression in ECs.

### Statistical Analyses

All quantifications were done by at least two researchers who were blinded to the treatment groups on images that were coded. Data were analyzed using GraphPad Prism 6 by one-way

ANOVA followed with multiple comparisons and Tukey's correction. Survival rate was analyzed using log-rank test. Data are presented as mean  $\pm$  standard deviation (SD). A *P* value of 0.05 was considered significant. Sample sizes were estimated based on a  $\alpha=0.05$  and 80% power, with effect sizes and sample variabilities estimated from our published studies [5, 7] and were indicated in the figure legends.

Please see Online Data Supplement of Detailed Materials and Methods.

## RESULTS

### BMDEC specific *Alk1* deletion caused bAVM and *Alk1*<sup>-/-</sup> BMDECs present in bAVM lesion

We showed previously that *Eng*<sup>+/-</sup> BM causes cerebral capillary abnormalities of WT mice [13]. To test whether mutation of *Alk1* in BMDECs alone causes bAVM, we transplanted the BM collected from *PdgfbiCreER;Alk1<sup>2i/2f</sup>;Ai14<sup>+/-</sup>* mice to lethally irradiated 8-week-old WT mice (Fig. 1A). Brain AVM was induced by intra-brain injection of an adeno-associated viral vector expressing vascular endothelial growth factor [AAV-VEGF, 2 $\times$ 10<sup>9</sup> genome copies (gcs)] 4 weeks after the BM transplantation when recipients' BMs were fully reconstituted by donors' BMs (Supplementary Fig. 1). TM (2.5 mg/25g of body weight) was injected i.p. 2 weeks later when a fraction of BM derived cells had differentiated into ECs in brain angiogenic region [12, 13] to delete *Alk1* gene in BMDECs (Fig. 1A).

Latex dye casting bAVMs were developed in 4 of the 10 mice with *PdgfbiCreER;Alk1<sup>2i/2f</sup>;Ai14<sup>+/-</sup>* BM (Fig. 1B). Arteriovenous (AV) shunts were also detected in the intestines in 5 of the 9 mice with *PdgfbiCreER;Alk1<sup>2i/2f</sup>;Ai14<sup>+/-</sup>* BM (Supplementary Fig. 2) after TM administration. Mice with *PdgfbiCreER;Alk1<sup>2i/2f</sup>;Ai14<sup>+/-</sup>* BM had a higher vessel density (*p*=0.002) and more dysplasia vessels (*p*<0.001) than mice with WT BM (Fig. 1C & D). BMDECs were detected in bAVM lesion (Fig. 1E). About 28 $\pm$ 10.6% ECs in bAVM lesion were BMDECs. Only 3.8 $\pm$ 3.6% ECs in the contralateral side of brain were BMDECs (*p*=0.009, Supplementary Fig. 3) These data indicate that mutation of *Alk1* gene in BMDECs alone is sufficient to cause bAVM development.

### *Alk1*<sup>-/-</sup> ECs undergo clonal expansion in bAVMs

We found previously that proliferating *Alk1*<sup>-/-</sup> ECs are preferentially cluster in bAVM vessels [7]. This finding spurs us an idea that the small numbers of ECs with biallelic loss of *ALK1* can clonally overpopulate in bAVM. Brain AVMs were induced in 8 weeks old *PdgfbiCreER;Alk1<sup>2i/2f</sup>;confetti<sup>+/-</sup>* mice through intra-brain injection of AAV-VEGF (2 $\times$ 10<sup>9</sup> gcs) to induce brain focal angiogenesis followed by i.p. injection of TM (2.5 mg/25g of body weight) 2 weeks later (Fig. 2A). TM treatment will induce *Alk1* gene deletion and confetti locus activation in ECs. The confetti reporter irreversibly labels individual recombined ECs with one of the four fluorescent colors. Therefore, if a single EC clonally expands, we expect to see a cluster of ECs expressing same fluorescent color. Indeed, clusters of ECs expressing the same confetti colors were detected in bAVMs (Fig. 2B), but not in the contralateral hemisphere of the same mice (*Alk1*<sup>-/-</sup> ECs without VEGF treatment, Fig. 2C) or in the brains of TM treated *PdgfbiCreER;confetti<sup>+/-</sup>* mice around AAV-VEGF injection sites (WT ECs with VEGF treatment, Fig. 3D). As it is statistically unlikely that the clusters

of ECs with the same confetti colors in bAVMs were the result of multiple independent Cre recombination events, the observed pattern indicates that *Alk1*<sup>-/-</sup> ECs were clonally expanded in bAVMs.

Although more Confetti<sup>+</sup> ECs were found in the bAVM lesions than in the contralateral *Alk1*<sup>-/-</sup> brains or WT brain angiogenic regions, there were about 60% of ECs lacking any confetti color (Fig. 2B). It is most likely due to ineffective recombination of the confetti allele induced by 2.5 mg/25g TM, because a half of this dose (1.25 mg/25g) had induced near 100% recombination of *Alk1* floxed alleles as evidenced by the lack of Alk1 protein expression in brain ECs and the development of bAVMs (Supplementary Fig. 4A & B).

### Equal numbers of Alk1<sup>+</sup> and Alk1<sup>-</sup> ECs were proliferating in bAVMs

We showed previously that more ECs were proliferating in bAVMs that have *Alk1* deletion in near 100% ECs than in brain angiogenic regions of WT mice [7]. However, it is not clear if Alk1<sup>+</sup> ECs are also proliferating in bAVMs. To answer this question, we created a mosaic of Alk1<sup>+</sup> and Alk1<sup>-</sup> ECs in bAVM by treating *Pdgfrb*CreER;*Alk1*<sup>2f/2f</sup> mice with a low dose of TM (0.01 mg/25g of body weight) 14 days after intra-brain injection of AAV-VEGF. Brain samples were collected at 14 days after TM treatment (Fig. 3A), sectioned and stained for Alk1 (to assess the degree of gene knockout) and CD31 (to mark all ECs) to validate the mosaic status. Alk1 expression in ECs was identified by co-localization of Alk1 and CD31 expression. Mice treated with this dose of TM had about 48.0±16.8% ECs were Alk1<sup>+</sup> ECs (Supplementary Fig. 5).

To analyze EC-proliferation in bAVM lesions with mosaic Alk1<sup>+</sup> and Alk1<sup>-</sup> ECs in mice treated with 0.01 mg/25g of body weight TM, we co-labelled brain sections with the proliferation marker Ki67, Erg (a pan-EC transcription factor), and Alk1 (to identify Alk1<sup>-</sup> and Alk1<sup>+</sup> ECs). We observed that 45±13.3% of Ki67<sup>+</sup> ECs were Alk1<sup>-</sup> ECs and 55±13.3% Ki67<sup>+</sup> ECs were Alk1<sup>+</sup> ECs (p=0.42, Fig. 3), indicating that Alk1<sup>+</sup> and Alk1<sup>-</sup> ECs have similar proliferation capacity in bAVMs.

### The burden of ALK1<sup>-</sup> ECs correlates with bAVM severity and mouse mortality

To determine whether there is an association between the number of Alk1<sup>-</sup> ECs and bAVM severity, *Pdgfrb*CreER;*Alk1*<sup>2f/2f</sup>;Ai14<sup>+/-</sup> mice were treated with a high dose (1.25 mg/25g of body weight) or a low dose of TM (0.01 mg/25g of body weight) 14 days after intra-brain injection of AAV-VEGF (Fig. 4A). As expected, high dose TM treatment resulted in a greater degree of Cre recombination and *Alk1* deletion in ECs (based on the numbers of Ai14<sup>+</sup> and Alk1<sup>-</sup> ECs). Mice treated with the low dose TM had fewer Ai14<sup>+</sup> ECs than mice treated with the high dose TM in the bAVM lesions (61±20% vs. 87%±5%, P=0.01, Fig. 4B and C). The TM-vehicle (corn oil) treated mice also showed a low (but not zero) degree of recombination (29±10%), possibly due to Cre leakiness (Fig. 4B and C). The mice in the low TM group have more Alk1<sup>+</sup> ECs identified by immunostaining in bAVM lesions (48.0±16.8%) than mice in the high TM group (2.3±4.34%, P<0.001). Almost all ECs in the vehicle treated mice were Alk1<sup>+</sup> (99 ±8.25%, Fig. 4D & E). Mice in the high TM group also expressed a lower level of Alk1 protein in bAVM lesions (Supplementary Fig. 6).

We quantified dysplastic vessels (expressed as dysplasia index: number of vessels with lumens >15  $\mu$ m per 200 vessels) in bAVM lesions and counted the number of intestinal arteriovenous (AV) shunts using latex dye casting. We found that mice in the low TM dose group ( $4.5 \pm 1.1$ ) have fewer dysplastic vessels than mice in the high TM dose group ( $7.9 \pm 1.2$ ,  $P=0.001$ , Fig. 5A and B). No dysplastic vessel was found in the vehicle treated mice. Vessel densities were similar among groups (Fig. 5C). Large bAVM vessels (detected by latex dye casting) were present in 100% of mice treated with high TM dose, but only in 50% of low dose TM treated mice. No large bAVM vessels was detected in vehicle treated mice. The phenotype of low dose TM treated mice were analyzed 28 days after intra-brain injection of AAV-VEGF, which was 6 days later than mice in the high dose TM group. Increase of TM dose also increased the number of AV shunts and AV shunt penetrance in the intestines (Fig. 6A & B, and Table 1) and mouse mortality (Fig. 6C). Together, these data indicate that the burden of  $Alk1^{-}$  ECs correlates with AVM severity.

## DISCUSSION

In this paper, we show that mutation of *Alk1* gene in BMDECs caused bAVM and  $Alk1^{-}$  ECs were clonally expanded in mouse bAVM. Increasing TM dose increased the number of  $Alk1^{-}$  ECs in *PdgfbcreER;Alk1<sup>2f/2f</sup>;Ai14<sup>+/-</sup>* mice and the bAVM severity.

Several studies, including our own, support a role of BM-derived cells in bAVM development [13]. After VEGF stimulation in the brain, WT mice with *Eng<sup>+/-</sup>* BM developed a similar degree of cerebral capillary dysplasia as mice with *Eng<sup>+/-</sup>* somatic and BM cells, suggesting that loss of even one allele of *Eng* in BM-derived cells results in cerebrovascular dysplasia [13]. Conversely, *Eng<sup>+/-</sup>* mice transplanted with WT BM had fewer dysplastic capillaries than *Eng<sup>+/-</sup>* mice with *Eng<sup>+/-</sup>* BM, suggesting that BM-derived cells contribute to vascular malformations and that the tendency to form vascular malformation might be mitigated by transplantation of normal BM cells. However, it is not clear which type of BM cells play the central role in AVM development. More than 70% of BM derived cells differentiated into macrophages in brain angiogenic region while fewer than 7% of them differentiated into ECs [12, 13]. Previous studies showed that mutation of *Eng* or *Alk1* in ECs causes AVM development, and mutation of these genes in macrophage will not initiate AVM development [6, 7, 10]. Therefore, in this study, we tested if BMDECs are responsible for transmission of abnormal cerebrovascular phenotype. We transplanted the BM cells isolated from *PdgfbcreER;Alk1<sup>2f/2f</sup>;Ai14<sup>+/-</sup>* mice to lethally irradiated WT mice. Brain angiogenesis were induced after the BM of WT mice were reconstituted by *PdgfbcreER;Alk1<sup>2f/2f</sup>;Ai14<sup>+/-</sup>* BM. *Alk1* deletion was induced two weeks after the induction of brain angiogenesis when BM cells had homed to brain angiogenic region and a fraction of homed BM cells had differentiated into ECs (Fig. 1A). AVMs in the brains and AV shunts in the intestines developed in WT mice with *PdgfbcreER;Alk1<sup>2f/2f</sup>;Ai14<sup>+/-</sup>* BM. Our data demonstrate that BMDEC is an important cellular contributor among all BM cells in AVM development.

Analysis of human brain and lung AVMs in HHT patients indicated that haploinsufficiency of the HHT causative gene is not sufficient to cause AVM development [18]. Inactivation of the remaining WT allele appears to be required for lesion formation, irrespective of the

mechanism by which it is inactivated, e.g., loss-of-function somatic mutation of the WT allele or loss of protein during inflammation [19, 20]. In mice, the loss of a single allele of *Eng* or *Alk1* recapitulates certain aspects of the human disease, primarily in older animals [21, 22]. Brain AVM does not commonly develop in mice with haploinsufficiency of these genes. Loss of both alleles of any HHT-causative gene is embryonically lethal in mice [23, 24] and conditional (tissue/time-specific) homozygous deletion of *Eng* [19] or *Alk1* [25, 26] results in striking vascular malformations resembling the AVMs found in HHT.

Although it is known that deletion of AVM causative genes in ECs is essential for AVM development [6, 7, 10] and gene deletion in a small fraction of ECs can cause bAVM [5, 11], currently, it is not clear how a small fraction of ECs with *Alk1* or *Eng* deletion leads to bAVM. It is also not clear if all ECs with *Alk1* or *Eng* deletion in a bAVM are descended from one or a few ECs with *Alk1* or *Eng* deletion. Using mice with confetti reporter transgene, we observed that ECs expressing the same confetti color clustered in bAVM lesions. Each bAVM lesion had several EC-clusters that express different confetti reporters, suggesting that a bAVM can be developed by several ECs with *Alk1* deletion. This phenotype was not detected in brain angiogenic regions of WT mice, nor in the brains of mice with *Alk1* gene deletion alone. Our data suggest that *Alk1* mutant ECs in bAVMs undergo clonal expansion, which could partially explain why a fraction of *Alk1* mutant ECs can lead to bAVM development. Due to the high recombination rate of *Alk1* floxed allele (near 100%) and low recombination rate of confetti transgene in response to 2.5 mg/25g of body weight TM treatment, we could not analyze if WT ECs are also clonally expanding in our AVMs model. We will consider using a different reporter line that is more effective in recombination to address this question in the future [27].

We showed previously that deletion of *Alk1* gene in ECs in the adult brain increased EC-proliferation in response to VEGF stimulation [7]. *Alk1* gene was deleted in almost all ECs in that study. AVM vessels had more proliferating ECs than the surrounding normal capillaries. Jin et al. showed that deletion of *Eng* in ECs in neonates resulted in more proliferating *Eng*<sup>-</sup> ECs than WT ECs in bAVM lesions [14]. In our study, using an adult mouse model with a mosaic pattern of *Alk1*<sup>-</sup> and *Alk1*<sup>+</sup> ECs, we found that equal numbers of *Alk1*<sup>+</sup> and *Alk1*<sup>-</sup> ECs were proliferating in bAVM lesions. Our data suggest that the *Alk1*<sup>-</sup> ECs may promote the growth of surrounding *Alk1*<sup>+</sup> ECs. Similarly, the clonal analysis of the mosaic retinal vasculature of *Eng* knockout mice revealed an equal proliferation rate of *Eng*<sup>+</sup> and *Eng*<sup>-</sup> ECs in AVMs vessels in the retina, although more *Eng*<sup>-</sup> ECs were proliferating in the vessels outside of AVMs, suggesting that non-cell autonomous mechanisms contributes to the expansion of AVMs [14]. It has been shown previously that *Alk1*<sup>-/-</sup> embryos expressed higher levels of angiogenic factors than *Alk1*<sup>+/-</sup> and *Alk1*<sup>+/+</sup> embryos [28]. Therefore, *Alk1*<sup>-</sup> ECs in bAVM could stimulate surrounding WT EC-proliferation through increasing the levels of angiogenic factors in the environment. The increased flow in AVM could also contribute to the increase of EC-proliferation and vascular remodeling in the lesions [29, 30]. However, the role of WT ECs in bAVM pathogenesis remains to be elucidated.

We also evaluated the relationship between the number of *Alk1*<sup>-</sup> ECs and AVM severity. By titrating the TM dose, we were able to reduce the number of *Alk1*<sup>-</sup> ECs in

*PdgfbicreER;Alk1<sup>2f/2f</sup>;Ai14<sup>+/-</sup>* mice, and found that mice treated with a high dose of TM had more severe AVM phenotype than mice treated with a low dose of TM. Since most of the mice will die within 10 days after the high dose TM treatment, we collected tissues 8 days after TM treatment from this group to ensure that most of the treated mice were still alive at the time of sample collection. However, the phenotype of the low dose TM treated mice develops slower and is less severe than that of the high TM treated mice. We postponed the sample collection time from the low dose TM treated mice to ensure that significant AVM phenotype can be detected. Although the samples were collected at different time points, our conclusion was not affected, because even the low dose TM treated mice had 6 more days than the high dose TM treated mice to develop AVM phenotype, these mice still showed less severe phenotype than that in the high dose group. It is consistent with our conclusion that reduction of TM dose reduced the AVM severity. These data suggest that novel therapeutic strategies, such as transfusion of normal circulating ECs or overexpression of Alk1 gene [31], that can reduce the burden of mutant ECs could potentially alleviate AVM phenotype severity in HHT patients.

In summary, we showed that *Alk1* deletion in BMDECs causes bAVM development and that Alk1<sup>-</sup> ECs were clonally expanded in the bAVMs. The proportion of Alk1<sup>-</sup> ECs is positively correlated with AVM phenotype severity. Together, our data suggest that reduction of Alk1<sup>-</sup> ECs in bAVM lesions can be a target for developing new therapies to alleviate the severity of bAVMs in HHT patients.

## Supplementary Material

Refer to Web version on PubMed Central for supplementary material.

## ACKNOWLEDGEMENTS

We thank Dr. Ludmila Pawlikowska for assistance with manuscript preparation.

### Funding

This study was supported by grants to H.S. from the National Institutes of Health (R01 HL122774, NS027713 and NS112819) and from the Michael Ryan Zodda Foundation. N.S. is supported by AHA fellowship (20POST35120371).

## Availability of data and material

The authors declare that all data supporting the findings of this study are available in the paper and its Supplementary Information.

## REFERENCES

1. Gauden AJ, McRobb LS, Lee VS, Subramanian S, Moutrie V, Zhao Z, et al. Occlusion of Animal Model Arteriovenous Malformations Using Vascular Targeting. *Transl Stroke Res.* 2020;11(4):689–99. [PubMed: 31802427]
2. Pan P, Weinsheimer S, Cooke D, Winkler E, Abla A, Kim H, et al. Review of treatment and therapeutic targets in brain arteriovenous malformation. *J Cereb Blood Flow Metab.* 2021:271678X211026771.



3. Bharatha A, Faughnan ME, Kim H, Pourmohamad T, Krings T, Bayrak-Toydemir P, et al. Brain arteriovenous malformation multiplicity predicts the diagnosis of hereditary hemorrhagic telangiectasia: quantitative assessment. *Stroke*. 2012;43(1):72–8. [PubMed: 22034007]
4. Kim H, Su H, Weinsheimer S, Pawlikowska L, Young WL. Brain arteriovenous malformation pathogenesis: a response-to-injury paradigm. *Acta Neurochir Suppl*. 2011;111:83–92. [PubMed: 21725736]
5. Walker EJ, Su H, Shen F, Choi EJ, Oh SP, Chen G, et al. Arteriovenous malformation in the adult mouse brain resembling the human disease. *Ann Neurol*. 2011;69(6):954–62. [PubMed: 21437931]
6. Choi EJ, Chen W, Jun K, Arthur HM, Young WL, Su H. Novel brain arteriovenous malformation mouse models for type 1 hereditary hemorrhagic telangiectasia. *PLoS One*. 2014;9(2):e88511. [PubMed: 24520391]
7. Chen W, Sun Z, Han Z, Jun K, Camus M, Wankhede M, et al. De novo cerebrovascular malformation in the adult mouse after endothelial Alk1 deletion and angiogenic stimulation. *Stroke*. 2014;45(3):900–2. [PubMed: 24457293]
8. Zhu W, Saw D, Weiss M, Sun Z, Wei M, Shaligram S, et al. Induction of Brain Arteriovenous Malformation Through CRISPR/Cas9-Mediated Somatic Alk1 Gene Mutations in Adult Mice. *Transl Stroke Res*. 2019;10(5):557–65. [PubMed: 30511203]
9. Chen W, Choi EJ, McDougall CM, Su H. Brain arteriovenous malformation modeling, pathogenesis, and novel therapeutic targets. *Transl Stroke Res*. 2014;5(3):316–29. [PubMed: 24723256]
10. Garrido-Martin EM, Nguyen HL, Cunningham TA, Choe SW, Jiang Z, Arthur HM, et al. Common and distinctive pathogenetic features of arteriovenous malformations in hereditary hemorrhagic telangiectasia 1 and hereditary hemorrhagic telangiectasia 2 animal models--brief report. *Arterioscler Thromb Vasc Biol*. 2014;34(10):2232–6. [PubMed: 25082229]
11. Choi EJ, Walker EJ, Shen F, Oh SP, Arthur HM, Young WL, et al. Minimal homozygous endothelial deletion of Eng with VEGF stimulation is sufficient to cause cerebrovascular dysplasia in the adult mouse. *Cerebrovasc Dis*. 2012;33(6):540–7. [PubMed: 22571958]
12. Hao Q, Liu J, Pappu R, Su H, Rola R, Gabriel RA, et al. Contribution of bone marrow-derived cells associated with brain angiogenesis is primarily through leukocytes and macrophages. *Arterioscler Thromb Vasc Biol*. 2008;28(12):2151–7. [PubMed: 18802012]
13. Choi EJ, Walker EJ, Degos V, Jun K, Kuo R, Pile-Spellman J, et al. Endoglin deficiency in bone marrow is sufficient to cause cerebrovascular dysplasia in the adult mouse after vascular endothelial growth factor stimulation. *Stroke*. 2013;44(3):795–8. [PubMed: 23306322]
14. Jin Y, Muhl L, Burmakin M, Wang Y, Duchez AC, Betsholtz C, et al. Endoglin prevents vascular malformation by regulating flow-induced cell migration and specification through VEGFR2 signalling. *Nat Cell Biol*. 2017;19(6):639–52. [PubMed: 28530660]
15. Livet J, Weissman TA, Kang H, Draft RW, Lu J, Bennis RA, et al. Transgenic strategies for combinatorial expression of fluorescent proteins in the nervous system. *Nature*. 2007;450(7166):56–62. [PubMed: 17972876]
16. Schepers AG, Snippert HJ, Stange DE, van den Born M, van Es JH, van de Wetering M, et al. Lineage tracing reveals Lgr5+ stem cell activity in mouse intestinal adenomas. *Science*. 2012;337(6095):730–5. [PubMed: 22855427]
17. Park SO, Lee YJ, Seki T, Hong KH, Fliess N, Jiang Z, et al. ALK5- and TGFBR2-independent role of ALK1 in the pathogenesis of hereditary hemorrhagic telangiectasia type 2 (HHT2). *Blood*. 2008;111(2):633–42. [PubMed: 17911384]
18. Bourdeau A, Cymerman U, Paquet ME, Meschino W, McKinnon WC, Guttmacher AE, et al. Endoglin expression is reduced in normal vessels but still detectable in arteriovenous malformations of patients with hereditary hemorrhagic telangiectasia type 1. *Am J Pathol*. 2000;156(3):911–23. [PubMed: 10702408]
19. Mahmoud M, Allinson KR, Zhai Z, Oakenfull R, Ghandi P, Adams RH, et al. Pathogenesis of arteriovenous malformations in the absence of endoglin. *Circ Res*. 2010;106(8):1425–33. [PubMed: 20224041]
20. Snellings DA, Gallione CJ, Clark DS, Vozoris NT, Faughnan ME, Marchuk DA. Somatic Mutations in Vascular Malformations of Hereditary Hemorrhagic Telangiectasia Result in Bi-allelic Loss of ENG or ACVRL1. *Am J Hum Genet*. 2019;105(5):894–906. [PubMed: 31630786]

21. Srinivasan S, Hanes MA, Dickens T, Porteous ME, Oh SP, Hale LP, et al. A mouse model for hereditary hemorrhagic telangiectasia (HHT) type 2. *Hum Mol Genet.* 2003;12(5):473–82. [PubMed: 12588795]
22. Bourdeau A, Faughnan ME, Letarte M. Endoglin-deficient mice, a unique model to study hereditary hemorrhagic telangiectasia. *Trends Cardiovasc Med.* 2000;10(7):279–85. [PubMed: 11343967]
23. Urness LD, Sorensen LK, Li DY. Arteriovenous malformations in mice lacking activin receptor-like kinase-1. *Nat Genet.* 2000;26(3):328–31. [PubMed: 11062473]
24. Sorensen LK, Brooke BS, Li DY, Urness LD. Loss of distinct arterial and venous boundaries in mice lacking endoglin, a vascular-specific TGFbeta coreceptor. *Dev Biol.* 2003;261(1):235–50. [PubMed: 12941632]
25. Milton I, Ouyang D, Allen CJ, Yanasak NE, Gossage JR, Alleyne CH Jr., et al. Age-dependent lethality in novel transgenic mouse models of central nervous system arteriovenous malformations. *Stroke.* 2012;43(5):1432–5. [PubMed: 22328553]
26. Park SO, Wankhede M, Lee YJ, Choi EJ, Fliess N, Choe SW, et al. Real-time imaging of de novo arteriovenous malformation in a mouse model of hereditary hemorrhagic telangiectasia. *J Clin Invest.* 2009;119(11):3487–96. [PubMed: 19805914]
27. Pontes-Quero S, Heredia L, Casquero-Garcia V, Fernandez-Chacon M, Luo W, Hermoso A, et al. Dual ifgMosaic: A Versatile Method for Multispectral and Combinatorial Mosaic Gene-Function Analysis. *Cell.* 2017;170(4):800–14 e18. [PubMed: 28802047]
28. Oh SP, Seki T, Goss KA, Imamura T, Yi Y, Donahoe PK, et al. Activin receptor-like kinase 1 modulates transforming growth factor- beta 1 signaling in the regulation of angiogenesis. *Proc Natl Acad Sci U S A.* 2000;97(6):2626–31. [PubMed: 10716993]
29. Corti P, Young S, Chen CY, Patrick MJ, Rochon ER, Pekkan K, et al. Interaction between alk1 and blood flow in the development of arteriovenous malformations. *Development.* 2011;138(8):1573–82. [PubMed: 21389051]
30. Chen Y, Ma L, Yang S, Burkhardt JK, Lu J, Ye X, et al. Quantitative Angiographic Hemodynamic Evaluation After Revascularization Surgery for Moyamoya Disease. *Transl Stroke Res.* 2020;11(5):871–81. [PubMed: 32056157]
31. Kim YH, Phuong NV, Choe SW, Jeon CJ, Arthur HM, Vary CP, et al. Overexpression of Activin Receptor-Like Kinase 1 in Endothelial Cells Suppresses Development of Arteriovenous Malformations in Mouse Models Of Hereditary Hemorrhagic Telangiectasia. *Circ Res.* 2020.

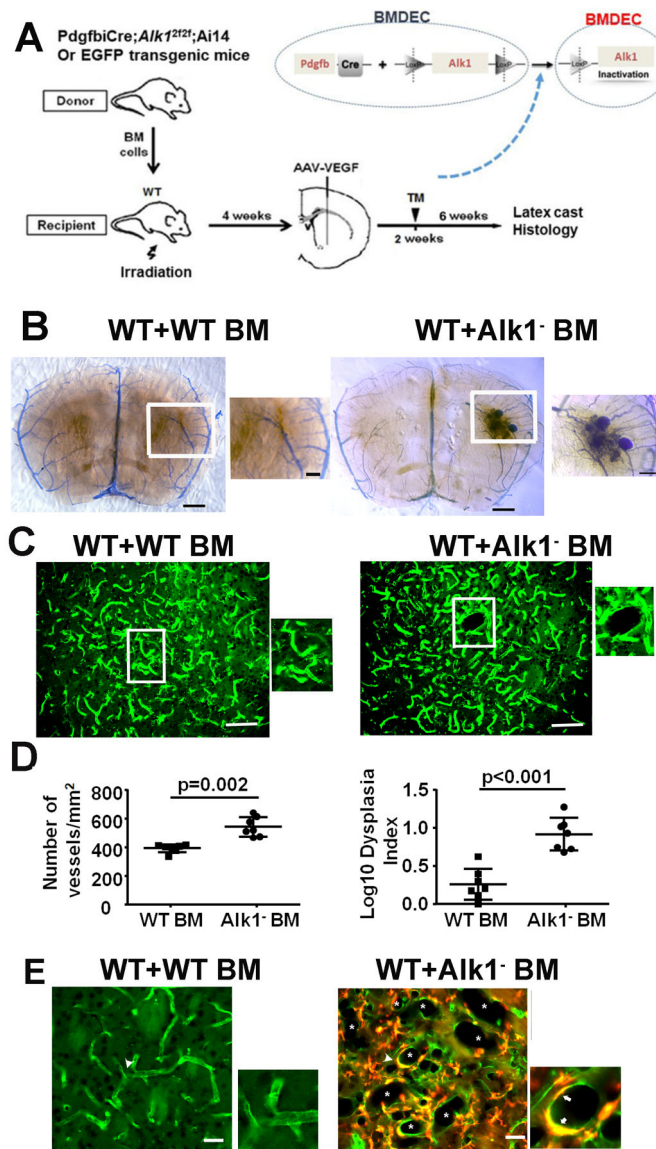


**Fig. 1. Mutation of *Alk1* in BMDECs caused bAVMs.**

**A.** Study design. BM collected from *Pdgbf1CreER;Alk1<sup>2f/2f</sup>;Ai14<sup>+/-</sup>* or EGFP transgenic mice were transplanted to lethally irradiated WT mice. AAV-VEGF ( $2 \times 10^9$  gcs) was injected to the brains of recipients 4 weeks after BM transplantation followed by TM (2.5 mg/25g of body weight) treatment 2 weeks later when a fraction of BM derived cells had differentiated into ECs in the brain angiogenic region to delete *Alk1* gene in BMDECs. AVM phenotype was analyzed 6 weeks after TM treatment by latex cast and histology. **B.** Image of latex perfused brain sections collected from a WT mouse with EGFP BM (WT+WT BM) and a WT mouse with *Pdgbf1CreER;Alk1<sup>2f/2f</sup>;Ai14<sup>+/-</sup>* BM (WT+Alk1 BM). Right: Enlarged image of the boxed area in the middle picture shows an AVM nidus. Scale bars: 1 mm for left and middle images, 200  $\mu$ m for the right image. **C.** Representative images of brain sections. The ECs were stained by intravascular perfused lectin (green). \*: dilated bAVM vessels. Scale bars: 100  $\mu$ m. **D.** Quantification of vessel density and Dysplasia

Index (number of abnormal vessels/200 vessels). Alk1 BM: WT mice transplanted with *Pdgfrb*CreER;*Alk1*<sup>2f/2f</sup>;Ai14<sup>+/-</sup> BM. WT BM: WT mice transplanted with EGFP BM. The numbers of dysplasia index were log transformed because they were not normally distributed. N=6. **E.** Microscopic image shows many dilated vessels (\*) in bAVM lesion. ECs were stained by intravascular perfused lectin (green). Recombined BMDECs expressed red fluorescent Ai14 reporter, therefore, they are yellow in the image. The two images on the right show two large vessels indicate by arrowheads in the left image that have clustered BMDECs (Arrows). Scale bar: 50  $\mu$ m.

Author Manuscript

Author Manuscript

Author Manuscript

Author Manuscript

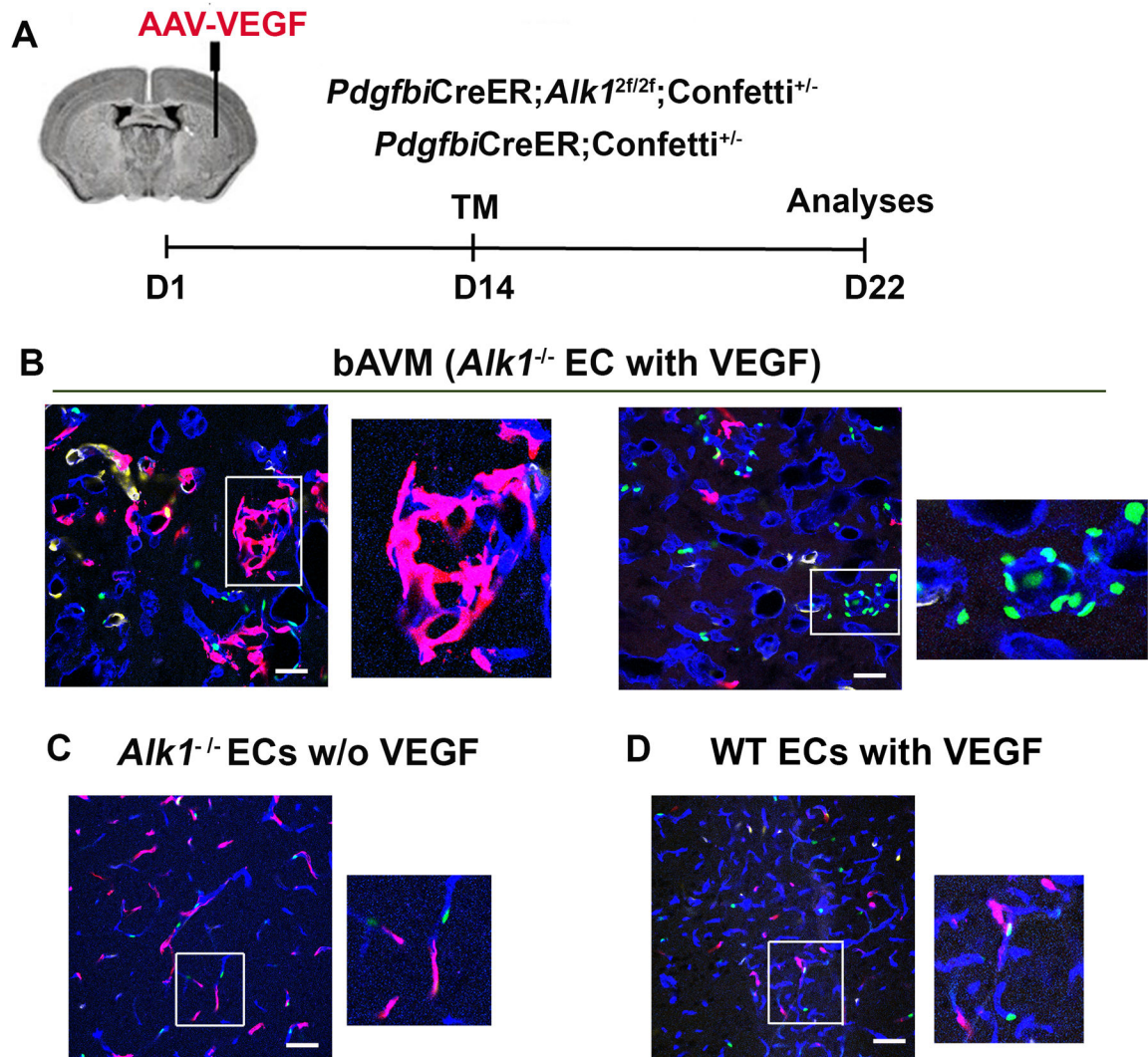


**Fig. 2. *Alk1*<sup>-/-</sup> EC clonally expanded in bAVM.**

**A.** Design. **B.** Confocal images show clusters of ECs expressing same confetti colors in bAVM lesions. Vessels were stained blue using an anti-CD31 antibody. Enlarged images of the rectangle regions in the left pictures show a cluster of RFP<sup>+</sup> ECs and a cluster of GFP<sup>+</sup> ECs in groups of abnormal vessels. **C.** Mouse brain with *Alk1* deleted in ECs without VEGF stimulation. **D.** WT mouse brain with VEGF stimulation. Enlarged images are the squared regions in **D** and **E** showing individual Confetti<sup>+</sup> ECs scattered in vessels. Scale bars: 50  $\mu$ m.

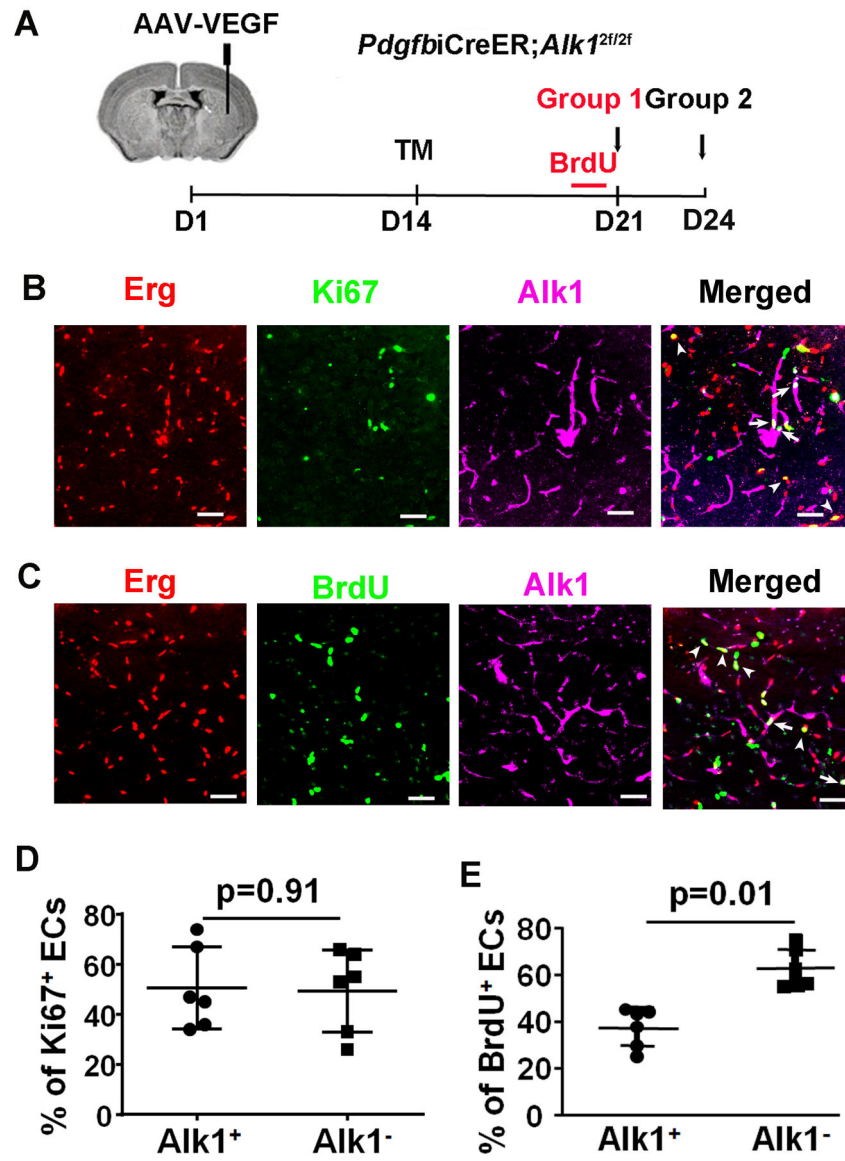


**Fig. 3. Equal numbers of Alk1<sup>+</sup> and Alk1<sup>-</sup> ECs were proliferating in the established bAVMs.**  
**A.** Design. **B.** Images of bAVM sections. The nuclei of ECs were stained by an Erg antibody (red). Proliferating cells were stained by a Ki67 antibody (green). Alk1 expression was stained by an Alk1 antibody (purple). Arrow: a Ki67<sup>+</sup> Alk1<sup>+</sup> EC. Arrowhead: a Ki67<sup>+</sup> Alk1<sup>-</sup> EC. Scale bars=50  $\mu$ m. **B.** Quantification of Ki67<sup>+</sup> Alk1<sup>-</sup> and Alk1<sup>+</sup> ECs. N=6.

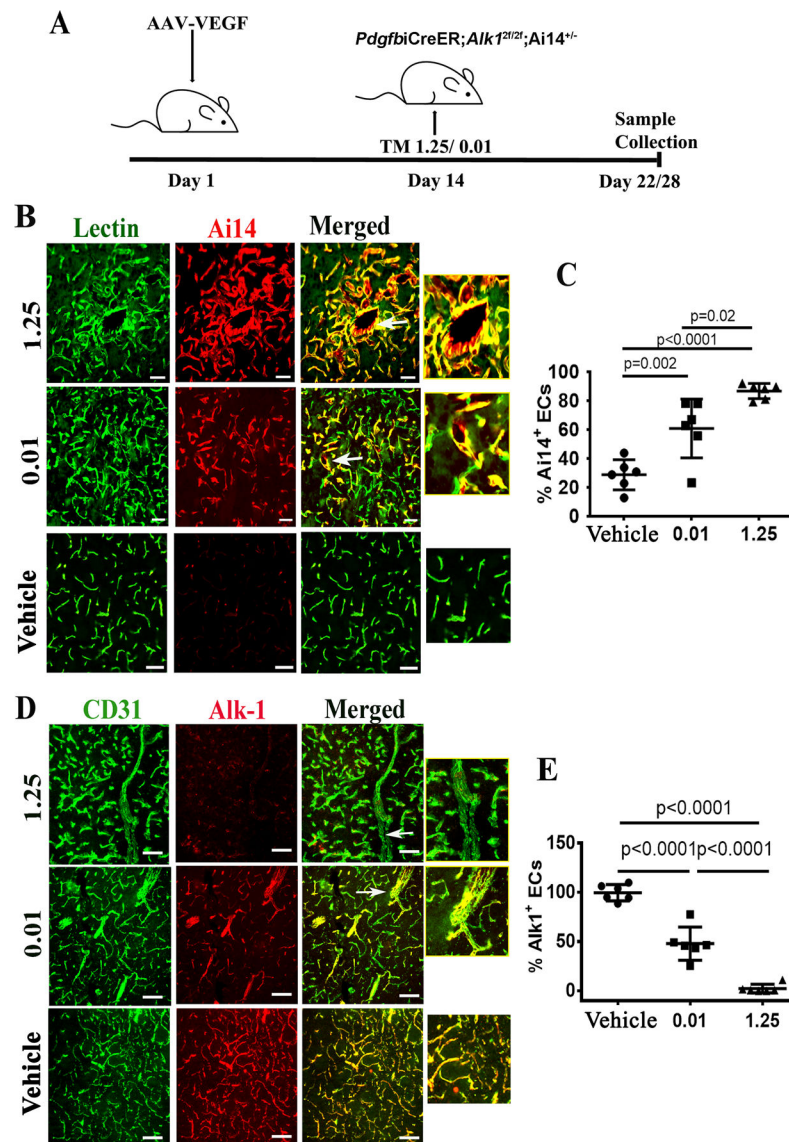


**Fig. 4: Increase of TM dose increased Ai14<sup>+</sup> and decreased Alk1<sup>+</sup> ECs.**

**A.** Design. TM 0.01/1.25: mice treated with 0.01 or 1.25 mg/25g of body weight TM. Day 22: samples were collected 22 days after intra-brain injection of AAV-VEGF from mice treated with high dose TM (1.25 mg/25g); Day 28: samples were collected 28 days after intra-brain injection of AAV-VEGF from mice treated with the low dose TM (0.01 mg/25g). **B.** Representative images of brain sections collected from lectin perfused mice. ECs were stained by intravascular perfused lectin (green). Cre activation in ECs was indicated by the expression of Ai14 reporter (red). Arrows indicate dysplastic vessels. Scale bars: 50  $\mu$ m. The right-side pictures show enlarged images of abnormal vessels indicated by arrows in the pictures on their left side. **C.** Quantification of Ai14<sup>+</sup> ECs in the bAVM lesions. **D.** Representative images of brain sections co-stained with anti-CD31 (green, ECs) and anti-Alk1 (red) antibodies. Arrows indicate abnormal vessels. Scale bar: 80  $\mu$ m. The right-side pictures show enlarged images of abnormal vessels indicated by arrows in the

pictures on their left side. **E.** Quantification of Alk1<sup>+</sup> ECs. WT: corn oil treated mice; 0.01 or 1.25: mice treated with 0.01 mg/25g or 1.25 mg/25g TM. N=6.

Author Manuscript

Author Manuscript

Author Manuscript

Author Manuscript



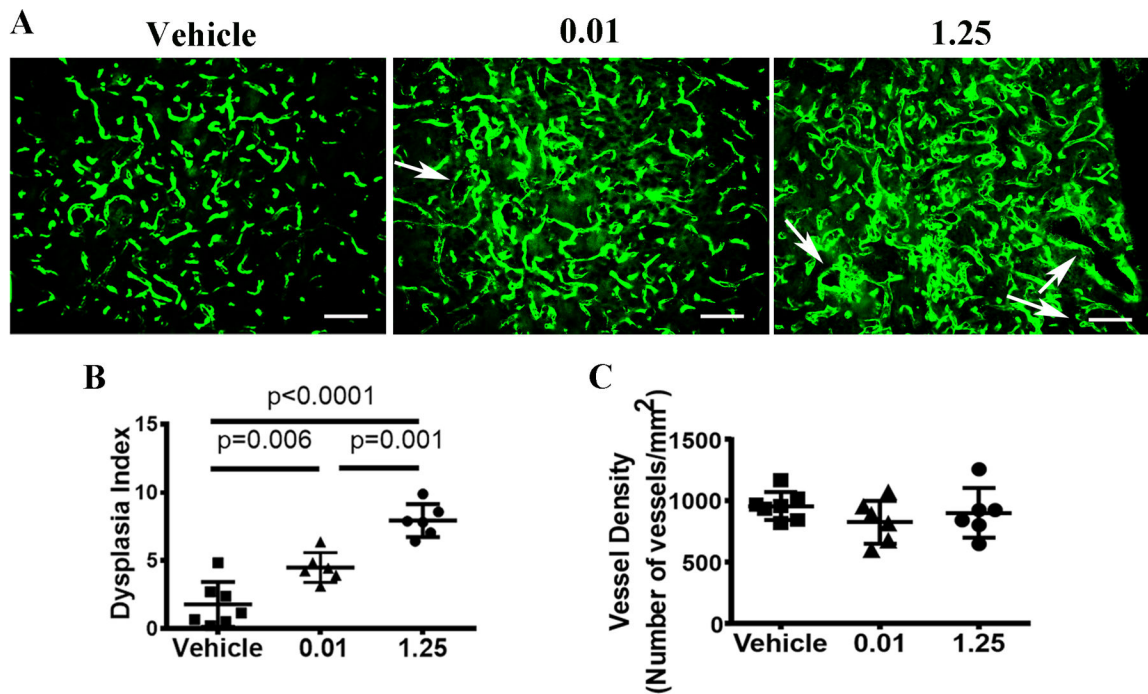


**Fig. 5. Reduction of the TM dose reduced the number of dysplastic vessels in bAVM lesions.**  
**A.** Representative images of brain sections. ECs were stained by intravascular perfused lectin (green). Arrows indicate dysplastic vessels. Scale bar: 80  $\mu$ m. **B.** Quantification of the Dysplasia Index. **C.** Quantification of vessel density. Vehicle: corn oil treated mice; 0.01 or 1.25: mice treated with 0.01 mg/25g or 1.25mg/25g TM. N=7 for the Vehicle group; N=6 for the 0.01 and 1.25 TM groups.

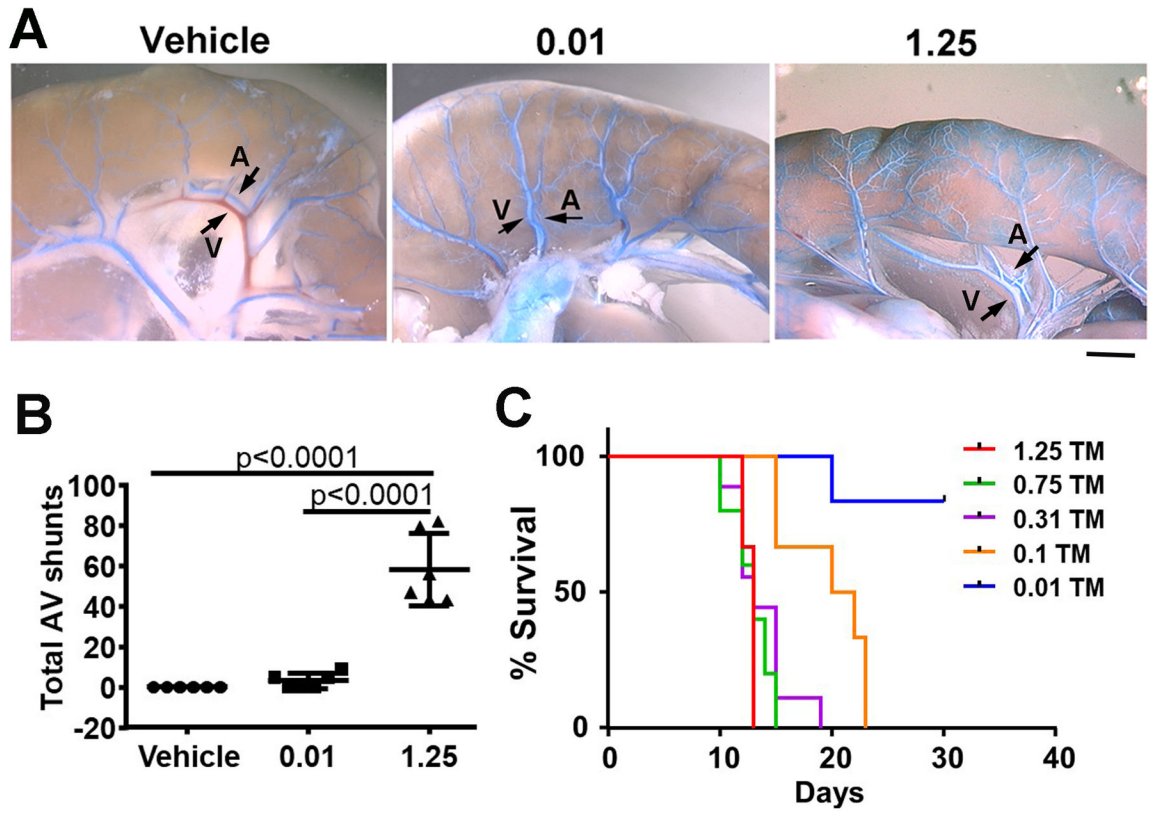


**Fig. 6. Reduction of TM dose reduced the number of AV shunts in the intestines and mouse mortality.**

**A.** Representative images show AV shunts in the intestines. The vessels were casted with latex dye (blue). Latex dye entered some veins of mice treated with 0.01 and 1.25 mg/25g TM after being injected into intra-left cardiac ventricles. Arrows indicate an artery (A) and a vein (V). Scale bar: 1 mm. **B.** Quantification of AV shunts. 0.01 and 1.25: mice treated with 0.01 or 1.25 mg/25g TM. Vehicle: mice treated with corn oil. **C.** The survival curve. Mice were treated with one i.p. injection of 1.25, 0.75, 0.3, or 0.1 mg/25g of body weight TM. N=6.

**Table 1.**

Penetrance of AV shunt in the intestines

1.25	0.01	Vehicle
100% (6/6)	50% (3/6)	0% (0/6)

Note: 1.25 and 0.01: mice treated with 1.25 or 0.01 mg/25g TM. Vehicle: mice treated with corn oil.

Author Manuscript

Author Manuscript

Author Manuscript

Author Manuscript